BEST AVAILABLE IMAGES

Defective images within this document are accurate representations of the original documents submitted by the applicant.

Defects in the images may include (but are not limited to):

- BLACK BORDERS
- TEXT CUT OFF AT TOP, BOTTOM OR SIDES
- FADED TEXT
- ILLEGIBLE TEXT
- SKEWED/SLANTED IMAGES
- COLORED PHOTOS
- BLACK OR VERY BLACK AND WHITE DARK PHOTOS
- GRAY SCALE DOCUMENTS

IMAGES ARE BEST AVAILABLE COPY.

As rescanning documents *will not* correct images, please do not report the images to the Image Problem Mailbox.

APPENDIX II

- *Effect of Sodium Deposition of FCC Catalysts Deactivation* by Tangstad et al., Applied Catalyst A: General 150 (1997) 85-99.
- *Pathways for Y Zeolite Destruction: The Role of Sodium and Vanadium*, by Xu et al., J. of Catalysis, 207, 237-246 (2002).
- *Effect of Vanadium on USY zeolite destruction in the presence of sodium ions and steam* by Hagiwara et al., Applied Catalysis A: General 249 (2003) 213-228.

Journal of Catalysis 207, 237–246 (2002)
doi:10.1006/jcat.2002.3517, available online at http://www.idealibrary.com on IDEAL®

Pathways for Y Zeolite Destruction: The Role of Sodium and Vanadium

Mingting Xu, Xinsheng Liu, and Rostam J. Madon[1]

Engelhard Corporation, 101 Wood Avenue, Iselin, New Jersey 08830

Received July 5, 2001; revised January 3, 2002; accepted January 3, 2002

A large amount of research in fluid catalytic cracking (FCC) has focused on understanding the destructive role of vanadium, since it is a major issue for catalyst performance during the cracking of residuum-containing feeds. Here, we establish a mechanism for the destruction of Y zeolite which ties the roles of sodium and vanadium together and explains their synergy. Understanding pathways for Y destruction is necessary to improve FCC performance. Y zeolite destruction in the presence of steam occurs via two pathways: steam hydrolysis of framework Al and direct attack by sodium species. For low Na^+ Y zeolite, steam hydrolysis of framework Al is the main cause of zeolite collapse. In such a pathway, rapid healing of framework tetrahedral holes by Si species from silica-enriched matrices stabilizes the zeolite. In the second pathway, sodium is responsible for zeolite hydrothermal instability. Sodium reacts with steam to form an active center, a surface NaOH, for zeolite destruction. All our observations are rationalized by proposing that the key to destruction lies in the ease of formation and availability of NaOH. It is the basic OH^- entity that attacks the framework Si–O bonds. Vanadium does not engender a new destructive pathway. At 970–1100 K in the presence of air and steam, V will be, as suggested by others, in a surface mobile state in an acidic form. This V species reacts with cationic sodium, facilitating its release from the Y exchange site. The sodium metavanadate thus formed hydrolyzes in steam to form NaOH and metavanadic acid, which may again react with Na^+ cations. Here, as in the V-free case, NaOH is the destructive agent, with formation of the basic OH^- entity again being the key. The role of vanadium is to catalyze and facilitate the formation of NaOH. And the mechanism of Y destruction, NaOH attacking Si–O, remains the same whether V is present or not. Without sodium, V itself has little effect on Y zeolite stability, regardless of zeolite unit cell size.

Key Words: fluid catalytic cracking catalysts; USY; Y zeolite stability; vanadium; sodium; hydrothermal stability; Y zeolite destruction.

1. INTRODUCTION

A fluid catalytic cracking (FCC) catalyst is a porous microsphere containing Y zeolite, active or inert matrix, and a silica or alumina binder. Y zeolite is the rate-controlling constituent during catalytic cracking; hence its stability is crucial during the rigors of the cracking process. Sodium, which is associated mainly with the zeolite, and vanadium, which is prevalent in heavy feeds, are well-known destructive agents for zeolites in the presence of steam. In order to improve stability of FCC catalysts, we need to understand issues that affect stability and to comprehend mechanisms of destruction.

Sodium reduces catalytic cracking activity by neutralizing Brønsted acid sites (1–3) and by irreversibly destroying Y zeolite in the presence of steam (4). Sodium also decreases gasoline research octane number (RON) (5, 6), but there are some beneficial effects (7, 8). Madon *et al.* (7) showed that an FCC catalyst containing 20% Y zeolite with 0.73 wt% Na_2O retained, after steaming, a higher unit cell size and more Brønsted acidity and was therefore more active for gas oil cracking than when the Na^+ was decreased via ammonium exchange to 0.05 wt% Na_2O. Though steamed Y surface area decreased for the higher Na^+-containing catalyst, it still had higher activity. It also showed a decrease in dry gas and coke yields, and an increase in gasoline yield but with lower octane number. The latter result is consistent with the work of Brown *et al.* (5) and Pine *et al.* (6). Sodium cations on Y mimic rare earth cations in that they slow down dealumination during steaming. Therefore cationic sodium can affect product selectivity due to its influence on unit cell size (ucs) during steaming and hence on Brønsted acid site density. Noncationic sodium deposited on the catalyst decreases activity with no effect on selectivity (7, 8).

Vanadium species, deposited on FCC catalysts from porphyrin complexes in crude oil during cracking, help destroy Y zeolite in FCC regenerators. One hypothesis put forth by Wormsbecher *et al.* (9) suggests that vanadium reacts with steam to form volatile vanadic acid in high-temperature oxidizing conditions. The consequential acid-catalyzed hydrolysis of framework Al by vanadic acid results in irreversible loss of the zeolite. Trujillo *et al.* (10) counter this argument as follows: a typical FCC feed contains 1 wt% sulfur, and about one-fourth of such sulfur is incorporated into coke and carried into the regenerator, where it is oxidized to SO_x. Thus the minimum concentration of SO_3 or sulfuric acid in the regenerator would be about 60 ppm, at least an order of magnitude greater than for vanadic acid. Trujillo *et al.* query that if the mechanism of Y zeolite

[1] To whom correspondence should be addressed. E-mail: Rostam.Madon@Engelhard.com.

0021-9517/02 $35.00

destruction by vanadium is via acid-catalyzed hydrolysis of framework aluminum, then why would such hydrolysis be caused by a weaker acid in lower concentration and not by the stronger and more abundant sulfuric acid? Trujillo *et al.* attribute this phenomenon to high local concentration of vanadic acid inside the zeolite.

This proposed role of vanadic acid is inconsistent with some important observations. Pine (11) indicated that there was synergy between the destructive actions of sodium and vanadium and demonstrated that without sodium, vanadium itself had little effect on zeolite crystallinity. In particular, he found that the activation energy for the destructive process in the presence of sodium did not depend on the presence or absence of vanadium. Pine conducted his experiments on USY samples with low unit cell sizes, between 24.24 and 24.28 Å. Such zeolites have very low levels of framework Al, and therefore vanadium acid-catalyzed hydrolysis of framework aluminum is less likely to occur. One needs to ensure that Pine's observation is not related to unit cell size. We address this in our work. Pine proposed that sodium and vanadium both similarly catalyze the steam destruction of the zeolite framework. He suggested that, at least for zeolites with low ucs, steam destruction pathways other than framework Al hydrolysis may be responsible for zeolite destruction.

Our research focuses on and extends the current understanding of the destructive pathways for Y zeolites in the presence of sodium and vanadium. We propose two distinct pathways for zeolite destruction and establish a mechanism for destruction that explains the synergy between sodium and vanadium for USY hydrothermal stability.

2. EXPERIMENTAL METHODS

Table 1 lists the properties of our starting materials. The BET surface area of the entire sample minus the surface area for pores larger than 2 nm in diameter, obtained as a "*t*" plot, gives a microporous surface area which we assume, for convenience, tracks the zeolite surface area (ZSA). We performed unit cell size (ucs) measurements via X-ray diffraction using a Si standard. We measured sodium level by atomic absorption and bulk Si, Al, and V contents using X-ray fluorescence spectroscopy. The USY did not contain rare earth cations.

We measured Y zeolite acidity by pyridine adsorption using diffuse reflectance Fourier-transform infrared (FTIR) spectra. Detailed experimental procedures are described elsewhere (12). In this study, we report the number of Brønsted acid sites perturbed by pyridine at 453 K.

On selected V-containing samples, we carried out UV–visible diffuse reflectance spectroscopy on a Varian Cary 300 UV–visible spectrophotometer equipped with a diffuse reflectance attachment. The samples were loaded into a 2-mm high-quality quartz cuvette using barium sulfate as the reference material.

We made USY samples with different Na^+ levels by exchanging a Na–H–USY (properties shown in Table 1) with ammonia nitrate solution at a pH of 5. We dried the resulting materials at 363–373 K overnight followed by dry calcination in static air at 881 K for 1 h and studied hydrothermal stability by steaming the samples at 1060 K for 4 h in 1-atm steam.

In order to carry out stability studies on a highly siliceous, low sodium-containing USY sample, we used a material from TOSOH Corporation (Table 1). This material has an atomic bulk Si/Al ratio of 162 and a unit cell size of 2.426 nm. Because of its few exchange sites, various levels of sodium were added via incipient wetness. We used NaOH, $NaNO_3$, and $NaHCO_3$ as sodium sources. We measured zeolite surface area of the samples dried overnight at 358 K, then after calcination at 811 K for 2 h in static air, and finally after steaming at 1060 K.

We used Y-based FCC catalysts which were made using calcined kaolin microspheres (14). The final catalysts, after exchange with ammonium nitrate to remove sodium cations, contained 0.49 and 0.53 wt% Na_2O, respectively (Table 1). They contained no rare earth cations. We also made ultra low sodium FCC catalysts by further ammonium exchange of catalysts *A* and *B* and obtained Na_2O levels of 0.07 and 0.06 wt%, respectively.

We prepared vanadium-containing samples via incipient wetness using a cyclohexane solution of vanadium naphthenate following the procedure described by Mitchell (15). Resulting materials were dried and calcined at 894 K for 2 h in static air. For the TOSOH samples, we added vanadium via incipient wetness using aqueous solutions of NH_4VO_3 or $NaVO_3$.

TABLE 1

Physical and Chemical Properties of USY and Catalyst Samples

Property	Na–H–USY	High Si–USY (TOSOH)	FCC catalysts *A*	FCC catalysts *B*
Na_2O (wt%)	4.06	0.02	0.52	0.49
Total surface area (m^2/g)	621	703	301	369
Zeolite surface area (m^2/g)	551	555	115	249
Unit cell size (nm)	2.453	2.426	2.463	2.450
Framework Al/uc[a]	30	2	42	28
Bulk Si/Al (atomic)	2.63	162	0.63	1.45

[a] Calculated using the formula in Ref. (13).

3. RESULTS

3.1. *Effect of Sodium on the Stability of USY*

In order to study the effect of Na^+ on Y zeolite stability, we prepared several Y samples with Na_2O levels from 0.03 to 5.5 wt% by exchanging sodium out of or into our starting Na–H–USY sample containing 4.06% Na_2O. To study

thermal stability, we calcined these samples at 1060 K for 4 h in the absence of added water; to study hydrothermal stability, we steamed the samples at 1060 K for 4 h in 100% steam.

Figure 1A shows that under dry, thermal conditions, increasing the sodium level does not decrease USY stability; there is actually a slight improvement in stability. The small initial decrease in stability is due to the presence of adsorbed water on the USY samples. In contrast to thermal stability, hydrothermal stability of zeolite Y decreases rapidly with increasing Na^+ loading. We give the results of the steamed samples in Table 2 and also show the unit cell size trend in Fig. 1B. Samples *a* to *d* are labeled in Figs. 1A and 1B, and we note that as sodium levels increase, the steamed unit cell size is larger. Na^+ inhibits dealumination. Figure 1B shows that a linear relationship exists between steamed ucs and sodium content in a zeolite without other multivalent cations, such as rare earth cations. We can use this relationship to determine the percentage of sodium in the zeolite and matrix of FCC catalysts.

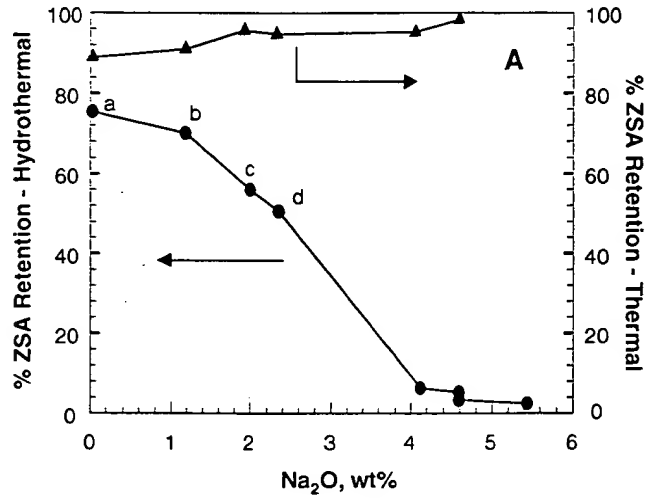

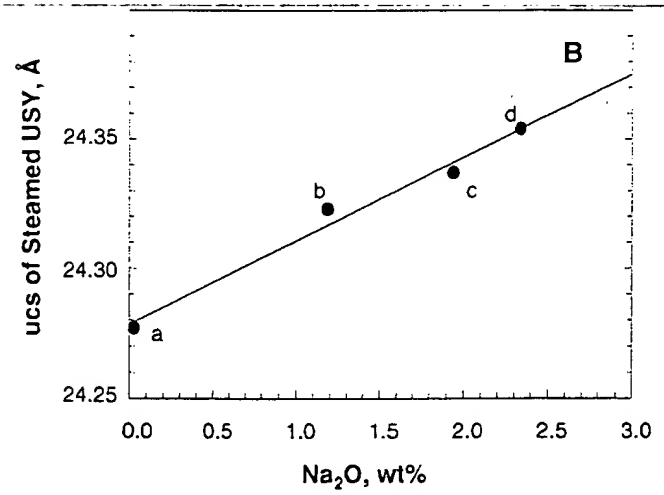

FIG. 1. (A) Stability of USY decreases with increasing Na^+ content under hydrothermal conditions but not under thermal conditions. Hydrothermal (steaming) conditions: 1 atm, 100% steam, 1060 K, 4 h. (B) Unit cell sizes of steamed USY (with no rare earth cations) versus Na_2O loading. Steaming conditions: 1060 K, 1 atm, 100% steam, 4 h.

TABLE 2

Properties of Steamed USY Zeolite with Respect to Sodium Content

Sample	Na_2O (wt%)	Initial Na^+/ unit cell	Steamed ucs (nm)	Steamed Al_F/uc	Steamed ZSA (m^2/g)	Brønsted acid site (μmol/g)
a	0.03	0.12	2.4277	4.2	457	58
b	1.19	4.7	2.4323	9.1	394	146
c	1.94	7.6	2.4337	10.6	305	163
d	2.34	9.2	2.4354	12.4	275	184
e	4.06[a]	16	—	—	35	29

[a] Starting Na–H–USY.

Sample *a* has high zeolite surface area retention after steaming, but since there is excessive dealumination the number of Brønsted acid sites is low. For sample *e*, at high levels of sodium, there is less dealumination but the surface area decreases dramatically; even though the ZSA is 13 times lower than that of sample *a*, the number of Brønsted acid sites are only twice as low. An optimum level of sodium maximizes Brønsted acidity, since the number of Brønsted acid sites per gram of catalyst depends on the total number of unit cells (i.e., the zeolite surface area) and on the number of framework aluminums (Al_F) per unit cell. The product of ZSA and number of Al_F/uc is roughly proportional to the number of Brønsted acid sites measured by FTIR.

This study demonstrates that the destruction of USY by sodium takes place only in the presence of steam and that *this destruction is not due to framework dealumination.*

To corroborate these results and to determine the pathway via which Na cations destroy USY, we carried out further investigations with a high Si–USY (Table 1) since here steam dealumination is no longer a factor for zeolite stability. This highly siliceous USY exhibits extremely high hydrothermal stability with no loss in surface area when steamed at 1060 K for 4 h.

We added different compounds of sodium, shown in Table 3, to high Si–USY via the incipient wetness technique. We first dried the samples and then calcined them. In samples containing sodium bicarbonate and sodium hydroxide, drying at only 358 K was sufficient to destroy ca. 25% of the zeolite. Further calcination at 811 K did not destroy any more zeolite. Sodium added via sodium nitrate solution was ineffective for Y destruction even at high Na levels.

Next, we varied the level of sodium bicarbonate on high Si–USY and calcined the samples under dry conditions (i.e., without added steam) at 811 K for 4 h. Figure 2 shows the substantial destruction of USY that occurs with just 0.78 wt% Na_2O. Indeed, 0.25 wt% Na_2O, which would correspond to only approximately 1 Na^+/uc, destroys ca. 65% of the zeolite crystallinity.

TABLE 3

Effect of Na_2O Added via Different Compounds on Zeolite Stability

High Si–USY	Na precursor			
	$NaHCO_3$	$NaNO_3$		NaOH
Na_2O (wt%)	0.19	0.29	0.67	0.19
Dried at 358 K/16 h				
ZSA (m^2/g)	401	547	533	404
ZSA retention (%)	72.3	98.7	96.3	73.0
Calcined at 811 K/2 h				
ZSA (m^2/g)	414	548	549	405
ZSA retention (%)	74.7	98.9	99.2	73.1

TABLE 4

Effect of Na_2O from $NaNO_3$ on Zeolite Stability[a]

Zeolite surface area (m^2/g)	Na_2O (wt%)				
	0.15	0.27	0.29	0.48	0.67
Dried at 358 K/16 h	—	—	547	—	533
Calcined at 811 K/2 h	559	557	548	557	549
With added water[a] and dried at 358 K/16 h	522	463	469	392	234

[a] Incipient wetness.

In order to understand the differences between the severe and immediate destruction caused by sodium bicarbonate and the relative ineffectiveness of sodium nitrate, we added water via incipient wetness to a *calcined* high Si–USY sample which initially contained $NaNO_3$. Now drying this sample at mild conditions of 358 K resulted in Y destruction (Table 4). Zeolite surface area decreased from 548 to 469 m^2/g at a Na_2O level of 0.29 wt%, and from 549 to 234 m^2/g at a Na_2O level of 0.67 wt%.

This enhanced effectiveness of $NaNO_3$ may be rationalized as follows. During calcination at 811 K, the sodium nitrate decomposes to a surface oxide. Making the catalyst incipiently wet allows formation of sodium hydroxide, which during the drying process destroys the zeolite. Comparing results in Tables 3 and 4 and Fig. 2, we note that more sodium nitrate is needed than $NaHCO_3$ and NaOH to destroy Y zeolite; we suggest that some of the surface sodium oxide made via $NaNO_3$ decomposition reacts with nonframework silica and is hence not available for Y destruction.

Finally, we examined the effect of adding $NaHCO_3$ via aqueous solution to a USY sample containing 0.03 wt% Na_2O, which we had steamed at 1060 K for 4 h in 100% steam to a ucs of 2.428 nm, similar to that of the high Si–USY. Compared to high Si–USY, this steamed sample has a large amount of nonframework Al with a bulk Si/Al ratio of 2.63. And, unlike the high Si–USY, this steamed USY shows excellent resistance to destruction via added sodium. For example, addition of 0.43 wt% Na_2O via $NaHCO_3$ followed by drying and calcination has no effect on zeolite stability (457 vs 448 m^2/g before and after sodium addition). This indicates that nonframework Al reacts with sodium and mitigates its destructive effects.

We conclude that the destruction of Y zeolite is related to the facility by which NaOH is available. Hydrolysis of sodium bicarbonate to the hydroxide takes place readily whereas $NaNO_3$ needs to be decomposed before NaOH can form. The availability of the basic entity OH^- is essential for Y destruction.

3.2. *Effect of Vanadium on the Stability of USY*

In Fig. 3 we show the hydrothermal stability of two USY samples containing Na_2O levels of 0.03 and 1.19 wt%, respectively, in the presence of different levels of vanadium.

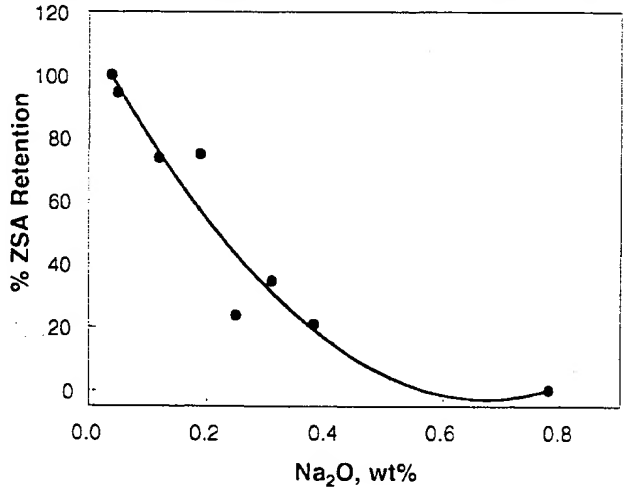

FIG. 2. Effect of sodium, added in the form of $NaHCO_3$, on the stability of high Si–USY. Conditions: dried at 358 K for 16 h followed by calcination at 811 K for 2 h.

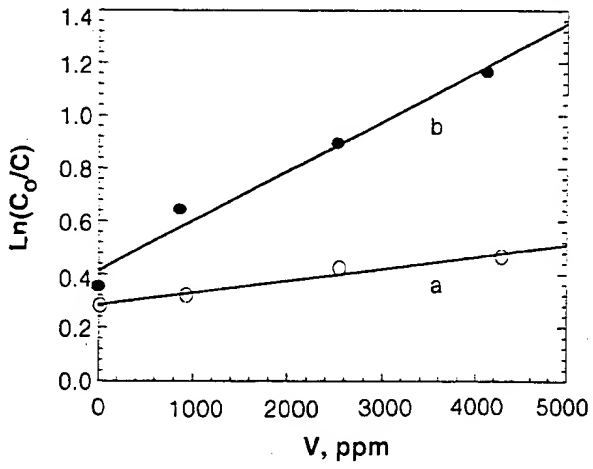

FIG. 3. Effect of vanadium on the rates of zeolite destruction at Na_2O levels of (a) 0.03 wt% and (b) 1.19 wt%. Steaming conditions: 1060 K, 1 atm, 90% steam/10% air, 4 h. C_0 is the zeolite surface area before steaming.

(These USY samples are the precursors to samples *a* and *b* in Table 2.) We follow hydrothermal stability with different levels of vanadium by plotting $\ln(C_0/C)$ versus vanadium level, where C_0 and C are zeolite surface areas before and after steaming; the ordinate, therefore, is a product of steaming time and a first-order rate constant for zeolite destruction. The larger the rate constant, i.e., the larger the slope, the less stable the zeolite.

For the USY sample containing 1.19 wt% Na_2O, the addition of vanadium causes a dramatic decrease in hydrothermal stability. The steamed Y surface area decreases from 394 m^2/g with no added vanadium to 175 m^2/g with 4200 ppm V, a 55% decline. For the sample with 0.03 wt% Na_2O, the addition of vanadium effects only a small decrease in hydrothermal stability. The steamed Y surface area decreases from 457 m^2/g with no added vanadium to 381 m^2/g with 4200 ppm V, only a 17% decline. In this sample, even after the addition of 4200 ppm V, the Y surface area of 381 m^2/g is close to that of the steamed 1.19% Na_2O sample containing no V. The net rate constant of zeolite destruction per 1000 ppm vanadium increases by about a factor of 5, from 0.01 to 0.05 h^{-1}, as Na_2O increases from 0.03 to 1.19 wt%. [Rate constant $k = 1/4 \times \ln(C_0/C)$, where 4 is steaming time in hours. The net rate constant at a particular sodium content is the rate constant in the presence of V minus the rate constant in the absence of V.]

The amount of sodium on the 1.19% Na_2O USY sample corresponds to the level found on commercial FCC catalysts. Since most FCC catalysts contain 20–40 wt% Y zeolite and 0.3–0.5 wt% Na_2O, and if all sodium is associated with zeolite, then the Na_2O content would correspond to 1.0–1.5 wt% per g of zeolite. But the location of sodium is important, and we use unit cell size as a guide. For example, 1.19 wt% Na_2O USY when steamed without any vanadium has a ucs of 2.432 nm (8.8 Al_F/uc), whereas the 0.03 wt% Na_2O USY, after steaming, has a ucs of 2.4277 nm (4 Al_F/uc). Since exchanged Na cations decrease hydrothermal dealumination, larger ucs values indicate increased levels of Na on zeolite exchange sites. Below we use two FCC catalysts to examine the importance of sodium content and location for the hydrothermal stability of Y in the presence of vanadium.

Table 1 shows the physical properties of the two FCC catalysts. In both cases, the sodium level exceeds 1 wt% per g of Y zeolite.

Figure 4 compares hydrothermal deactivation in the presence of vanadium for catalyst *A* and its lower Na analogue. For comparison, Fig. 4 also contains plots for the USY samples described earlier. Just as in the high-sodium USY case, for catalyst *A* containing 0.52 wt% Na_2O, the addition of vanadium causes a large decrease in hydrothermal stability. The steamed Y surface area decreases from 58 m^2/g with no added vanadium to 17 m^2/g with 4700 ppm V, a 70% decline. By lowering the sodium content of catalyst *A* to

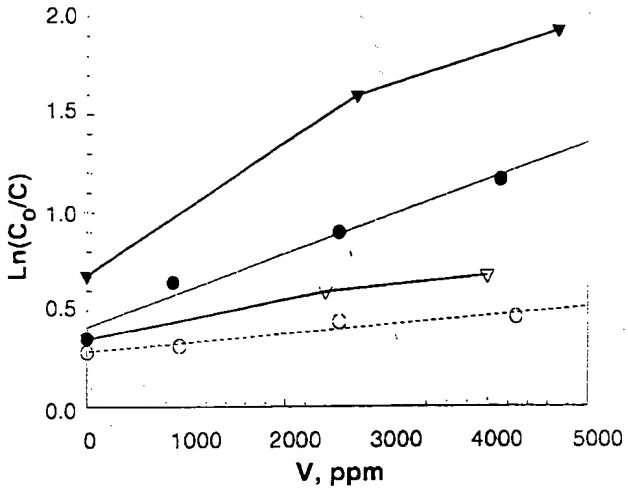

FIG. 4. Effect of vanadium on the hydrothermal stability of catalysts: ●, 1.19 wt% Na_2O/USY; ○, 0.03 wt% Na_2O/USY; ▼, ▽, FCC catalysts *A*, with 0.52 wt% Na_2O and 0.06 wt% Na_2O, respectively. Steaming conditions: 1060 K, 1 atm, 90% steam/10% air, 4 h.

0.06 wt% Na_2O, addition of vanadium has only a small effect on hydrothermal stability. The steamed Y surface area decreases from 80 m^2/g with no added vanadium to 54 m^2/g with 4000 ppm V, only a 27% decline. By decreasing Na content, the FCC catalyst, even after the addition of 4000 ppm V, has the same steamed surface area as catalyst *A* containing 0.52 wt% Na_2O and no vanadium.

The ucs of steamed catalyst *A* with 0.52 wt% Na_2O and no vanadium is 2.432 nm, whereas for the 0.06 wt% Na_2O analogue it is 2.4275 nm. This suggests that catalyst *A* contains a significant amount of exchanged Na and this consequently leads to substantial deactivation in the presence of vanadium. These ucs results are in line with the USY results of Fig. 4, indicating that the extent of Na^+ exchange on the Y zeolite and the deactivation results are consistent for the two samples.

Figure 5 compares hydrothermal deactivation in the presence of vanadium for catalyst *B* and its lower Na analogue. Again, for comparison, Fig. 5 contains plots for the USY samples described earlier. Here, unlike the previous cases, catalyst *B* with 0.49 wt% Na_2O does not show any substantial decrease in hydrothermal stability in the presence of vanadium. The steamed Y surface area decreases from 174 m^2/g with no added vanadium to 150 m^2/g with 4000 ppm V, only a 14% decline. By lowering the sodium content of catalyst *B* to 0.05 wt% Na_2O, there is no further improvement in vanadium tolerance. In this case, the steamed Y surface area decreases from 184 m^2/g with no added vanadium to 161 m^2/g with 4000 ppm V, a 13% decline.

Unlike the ucs of the steamed USY sample and catalyst *A*, the ucs of steamed catalyst *B* with 0.49 wt% Na_2O and no vanadium is low, 2.4275 nm, and for the 0.05 wt% Na_2O analogue it is the same. This indicates that for catalyst *B*, a

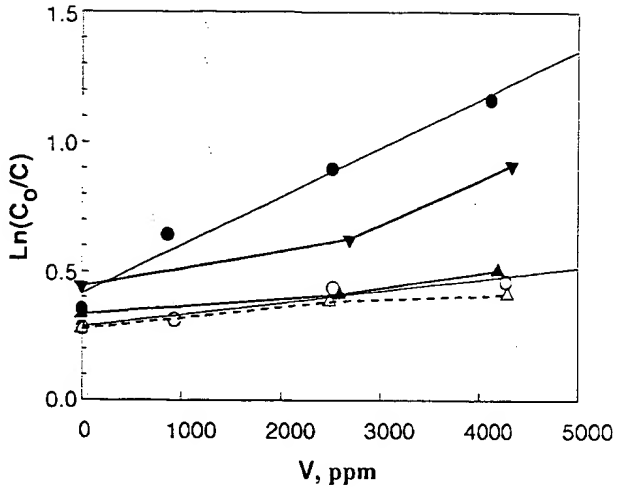

FIG. 5. Effect of vanadium on the hydrothermal stability of catalysts: ●, 1.19 wt% Na_2O/USY; ○, 0.03 wt% Na_2O/USY; ▲, △, FCC catalysts *B* with 0.49 wt% Na_2O and 0.05 wt% Na_2O, respectively; ▼, 0.95 wt% Na_2O, after Na^+ back-exchanged onto catalyst *B* (with 0.49% sodium). Steaming conditions: same as in Fig. 4.

substantial portion of the 0.49 wt% Na_2O is not on the zeolite exchange sites and is associated with the matrix. Since exchanged or available sodium is necessary to allow vanadium to be effective for destruction, we exchanged sodium back onto catalyst *B*. Now we see a distinct and large affect of vanadium on Y stability. Increasing Na_2O level from 0.49 to 0.95 wt% via sodium exchange with $NaNO_3$ solution decreases vanadium tolerance (Fig. 5). The surface area drops 37%, from 156 m^2/g at 0 ppm V to 98 m^2/g with 4000 ppm V. Note once again that the starting surface area of 156 m^2/g with no V present but after sodium exchange onto catalyst *B* is close to the surface areas with ca. 4000 ppm V when sodium is not available. These results confirm that for vanadium to be effective for Y destruction, sodium must be available, for example, on Y exchange sites, and it must not be locked in the matrix.

Besides sodium availability, the effect of vanadium is determined to a certain extent by whether it is trapped by matrix sites. Trujillo *et al.* (10) have suggested nonframework Al as being capable of trapping V, and matrices can be designed to trap vanadium. However in the presence of even small amounts of vanadium, sodium, if available, would contribute significantly to instability.

Since alumina-enriched matrix components play a role in enhancing stability, we concluded our study by using the highly siliceous, low-sodium TOSOH USY to investigate via model compounds the synergy between vanadium and sodium for zeolite destruction. We added ammonium metavanadate, sodium nitrate, and sodium metavanadate to the high Si–USY to obtain the levels of sodium and vanadium shown in Table 5.

All samples, even with vanadium levels greater than 7000 ppm, show excellent thermal stability. On steaming, the vanadium-only sample retains most of the zeolite surface area. The sample containing both sodium and vanadium is almost completely destroyed. We checked for V and Na retention on the samples and found no loss of vanadium or sodium after steaming. Figure 6 shows zeolite surface area retention after calcination and after steaming for the three samples.

TABLE 5

Effect of Sodium and Vanadium on the Stability of High Si–USY

	NH_4VO_3	$NaNO_3$	$NaVO_3$
Equivalent Na_2O (wt%)	0.02	0.51	0.48
Equivalent V (wt%)	0.80	0	0.72
ZSA (m^2/g)			
Dried at 358 K for 16 h	501	547	527
Calcined at 1060 K for 4 h	532	546[a]	503
Steamed at 1060 K for 4 h	436	188	33

[a] Sample was calcined at 810 K for 2 h.

We carried out UV–visible diffuse reflectance spectroscopy on the ammonium metavanadate, and on sodium metavanadate containing high Si–USY samples. USY, by itself, has no absorption bands at wavelengths above 350 nm; below 350 nm, very weak absorption bands at about 300, 240, and 205 nm are observed due to framework defects (spectra not shown). Figure 7 shows the results for both vanadium-containing USY samples after calcination and after steaming. The ammonium metavanadate-containing sample has absorption bands at 374, 290 (shoulder), 247, and 210 nm in its UV–visible spectrum after 1060 K calcination, while the calcined sample containing $NaVO_3$ has absorption bands at 389, 290, 250, and 210 nm. These bands are associated with O → V electron transfer (16, 17). Compared to pure NH_4VO_3 and $NaVO_3$ compounds, where we observe absorption bands around 368, 283, and 216 nm for NH_4VO_3, and 340, 280, and 216 nm for $NaVO_3$, the bands for the supported compounds are shifted toward the longer

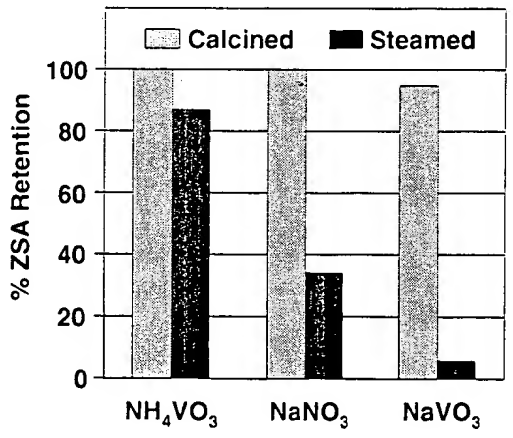

FIG. 6. ZSA retention after thermal (1060 K, 4 h) and hydrothermal treatments (1060 K, 1 atm, 90% steam/10% air, 4 h). High Si–USY impregnated with ammonium metavanadate, sodium nitrate, and sodium metavanadate.

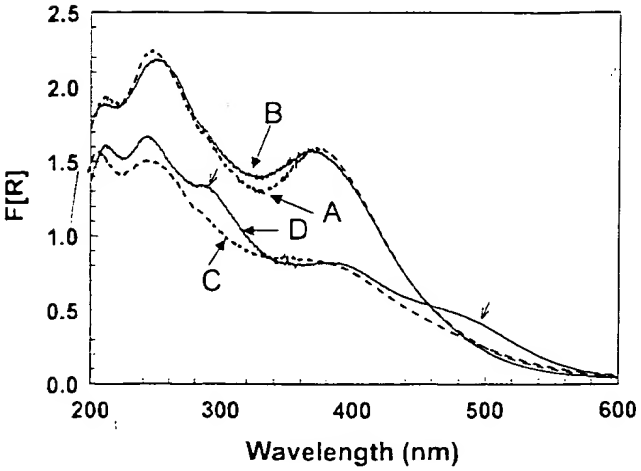

FIG. 7. UV-visible spectra of model vanadium compounds on high Si–USY. (A) Ammonium metavanadate on USY—calcined; (B) ammonium metavanadate on USY—steamed; (C) sodium metavanadate on USY—calcined; (D) sodium metavanadate on USY—steamed. (Treatment conditions given in Table 5.)

wavelengths. This spectral shift indicates that after calcination, the chemical environment of the metavanadates has changed from a pure compound form to a well-dispersed form where interactions of V with its surrounding occur via oxygen bridges. The V–O bond is shortened as a result of this. On steaming, we did not observe any significant spectral changes for the sample made with NH_4VO_3; it is in hydrogen form after calcination. However, steaming resulted in spectral changes for the sample made with $NaVO_3$. New bands at about 290 and 480 nm appeared, indicating the formation of V_2O_5 (10).

4. DISCUSSION

4.1. *Effect of Na^+ on Hydrothermal Stability of USY*

Hydrothermal deactivation of steam occurs via the hydrolysis and elimination of Al^{3+} from a tetrahedral site (18–20) of a Y zeolite. A substitution reaction in which available Si replaces an Al in the TOT site (19, 20) stabilizes the structure; if such a replacement does not take place, the segment of the zeolite would collapse. This represents one pathway for zeolite destruction, labeled A in Fig. 8. Removal of Al from the structure and its replacement by Si is accompanied by a shrinking of the unit cell. The destruction of zeolite via sodium also requires steam (Fig. 1A) but the mechanism is different.

As shown in Figs. 1A and 1B, there is a rapid decrease in zeolite retention for samples having Na^+/uc greater than ca. 4.7 (Fig. 1A), and the decrease in ucs after steaming is inversely proportional to the initial Na^+/uc on the starting material (Fig. 1B). If dealumination via steam (pathway A) was the only process leading to zeolite collapse, one would expect the opposite result, i.e., zeolites with high Na/uc would be more stable, since the hydrolysis–dealumination reaction only takes place at an Al–O–Si site which has a proton as the counterion (18). The destructive role of sodium is uniquely different from that of steam and is shown as pathway B in Fig. 8. In order to understand this pathway, we performed model studies with sodium compounds using the high Si–USY, where, due to there being only ca. 2 Al_F/uc, pathway A is not viable.

Results in Tables 3 and 4 and in Fig. 2 may be summarized as follows. Since sodium bicarbonate, a salt of a strong base and a weak acid, hydrolyzes readily at $\leq$358 K to give NaOH, ZSA retention in the presence of $NaHCO_3$ and NaOH (Table 3) is identical. Sodium nitrate does not hydrolyze readily and is ineffective. However, after it is decomposed at a higher temperature, the resulting surface sodium oxide reacts with added water at 358 K to form NaOH, and zeolite destruction takes place (Table 4). Formation of NaOH is the necessary step for the destruction of Y zeolite to take place via an OH^- attacking a Si–O bond (pathway B). The facility of attack is evident in that only a small amount of sodium is needed to cause significant destruction (Fig. 2). The important points therefore are the availability of sodium and the ease with which it forms NaOH. We need to relate these results to those in Fig. 1A and Table 2, i.e., where the deleterious effects of sodium occur in a high-temperature steam environment.

At low temperatures, NaOH in an aqueous phase would be solvated, and the presence of ionic species, Na^+ and OH^-, would offer a potent reaction environment for Y destruction. In high-temperature steam, at 1060 K, there is no solvation of NaOH and high ionic concentrations would be difficult to obtain. And though hydrolysis of a univalent cation in steam has been suggested (21), formation of NaOH via the hydrolysis of Na^+Y species with steam may also be difficult. Pine (11) found that the apparent activation energy of Y destruction with sodium is 79 kcal/mol and is independent of the Na concentration. Such a high value suggests that one or more kinetically significant steps are

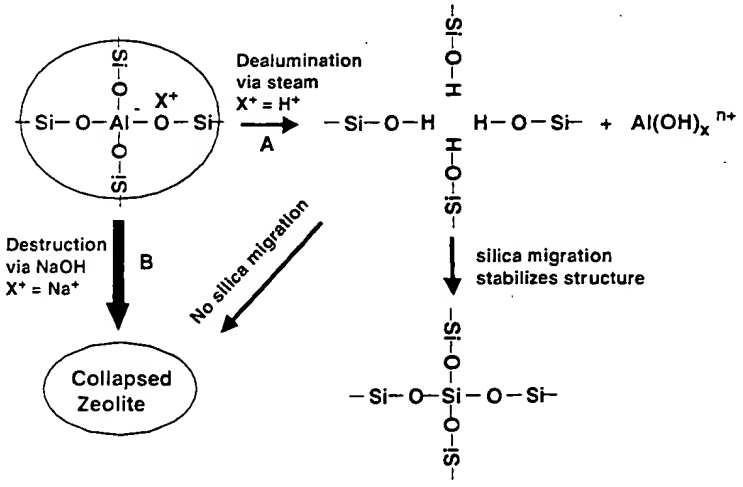

FIG. 8. Pathways to Y zeolite destruction.

energetically difficult steps in the reaction sequence. We will revisit this point later.

Before concluding this section, we suggest a second complementary pathway for NaOH formation in high-temperature steam besides hydrolysis of the cationic Na on Y. Rapid destruction of Y takes place when we have, for example, 5 Na^+/uc, which corresponds to 16% of the cationic sites in the unit cell. The other sites contain protons and are subject to dealumination and structural collapse. When a portion of the zeolite collapses, Na associated with that particular portion is no longer a strongly bonded entity. This Na readily reacts with steam to form NaOH. As further destruction takes place and more Na is available for hydrolysis, the destructive process continues. This case is similar to the $NaNO_3$ case (Table 4), where the nitrate needed to be decomposed before NaOH could form.

4.2. *Effect of V on the Hydrothermal Stability of USY*

The results on USY (Fig. 3) show that reducing Na_2O content from 1.19 to 0.03 wt% dramatically reduces the effect of V on Y stability and are consistent with Pine's results (11). The net rate constant of destruction for our 1.19 wt% Na_2O USY is 0.05 h^{-1} per 1000 ppm V. Pine (11) obtained a net rate constant of 0.025 h^{-1} per 1000 ppm V at 1033 K with an FCC catalyst containing 1.20 wt% Na_2O. Based on an activation energy of 79 kcal/mol (11), at 1060 K this net rate constant is 0.068 h^{-1} per 1000 ppm V. This value is remarkably similar to ours. The Al_F/uc of our USY is 30, ucs of 2.453 nm, whereas the USY used by Pine had a ucs of 2.423 nm with ca. $<1 Al_F$/uc. *The similar increase in the rate constant upon V addition for two USY materials with very different Al_F/uc indicates that vanadic acid-catalyzed hydrolysis of framework Al contributes little, if any, to zeolite instability.*

Figures 4 and 5 substantiate our results on USY and show that on FCC catalysts, besides the total amount of sodium in the catalyst, availability of that sodium is essential for destruction. For example, if sodium reacts with an amorphous matrix and is therefore unavailable, V will not play a role in Y destruction. For Y catalysts without rare earth cations, the unit cell size of steamed Y can indicate the location of sodium. In our case, catalyst *B* with a Na_2O content of 0.49 wt% has a steamed unit cell size of only 2.4275 nm, indicating that most of the sodium is not in cationic form on the zeolite. Its excellent stability in the presence of 4200 ppm V attests to the unavailability of sodium.

In order to construct a mechanism for Y destruction, our study using the low-sodium (0.02 wt% Na_2O), high Si–USY is instructive. This USY is extremely stable and does not lose any surface area when steamed at 1060 K. This is in line with pathway A in Fig. 8, which requires framework aluminum to be present for destruction to occur via steam.

Addition of model compounds to this USY shows that in the absence of steam neither ammonium metavanadate, sodium nitrate, nor sodium metavanadate is effective for Y destruction even at 1060 K. Ammonium metavanadate decomposes to ammonia and metavanadic acid at 473 K; the resulting metavanadic acid does not harm the zeolite at all in the absence of steam and is only marginally effective in steam, with 13% of the Y zeolite destroyed, even in an environment with 8000 ppm V. Though it is tempting to ascribe this low level of destruction to acid hydrolysis of framework Al, we suggest that it is due to the presence of the small amount of available Na^+ which is released in the presence of V.

Sodium nitrate decomposes to an oxide which again is ineffective without steam. In steam, as discussed earlier, the Na_2O forms NaOH, which is destructive and destroys 66% of the Y zeolite. This corresponds to pathway B in Fig. 8. After $NaNO_3$ decomposes, not all the sodium is available to form NaOH since some sodium reacts with the large amount of nonframework silica present on this high Si–Y.

Sodium metavanadate melts at 903 K, but without steam it does not harm the zeolite. The 5% decrease in ZSA during calcination is due to the small amount of steam released from the sample. This result refutes a proposal (22, 23) that low melting compounds of sodium and vanadium are detrimental to zeolite Y. When steam is present, 94% of the zeolite is destroyed. This large effect is reminiscent of our study (Fig. 2) with $NaHCO_3$, where facile hydrolysis of the bicarbonate to form NaOH was the key to Y destruction. Here sodium metavanadate reacts with steam to form NaOH and metavanadic acid. Unlike in the $NaNO_3$ case, all the sodium here is available to form NaOH; this results in the massive loss of zeolite Y. In the presence of sodium metavanadate and steam the pathway for Y destruction is pathway B in Fig. 8. *There is no separate pathway for zeolite destruction due to vanadium.*

4.3. *The Roles of Vanadium and Sodium in Y Destruction*

Pine (11) proposed that the role of vanadium and sodium was to catalyze the well-known destruction of zeolite by steam, and that both acted with nearly equal activity and with synergy. We have corroborated several of Pine's results and further have shown that the synergy between vanadium and sodium is present for both high- and low-ucs Y zeolites. To quote Pine: "The challenge is to devise a mechanism that can accommodate such chemically different species as catalysts to the same reaction and to explain why there is synergism between them."

Pine showed that the apparent activation energy for Y destruction is 76–79 kcal/mol. And though the overall first-order rate constant increases as either sodium or vanadium level increases (Figs. 3–5), the activation energy is not dependent on the sodium level and is the same whether vanadium is present or not. This latter fact indicates that the kinetically significant step for Y destruction does not include vanadium. We have proposed that the only destructive

pathways for Y zeolite are (a) dealumination by steam (pathway A) and (b) reaction with NaOH (pathway B). Pathway B is enhanced in the presence of vanadium, but the kinetic steps that describe this destruction are independent of vanadium.

The role of vanadium depends on the type of V compounds that are present at 1060 K in an environment containing oxygen and steam. There is consensus (9–11) that the relevant vanadium species exist in a +5 oxidation state. Under reaction conditions, it is reasonable that such species are acidic vanadium compounds (9, 10). There is some debate as to the exact nature of such species, but measurements in the literature (9, 10, 24–27) only indicate post reaction compounds on the catalyst surface devoid of the presence of steam and not those present under reaction conditions.

The sequence of steps below is an attempt to describe the role of vanadium. Though we do not know the exact intermediates at reaction conditions, we show these steps to emphasize the key feature of our proposal.

1. (a) $V_2O_5 + 3H_2O \rightleftarrows 2H_3VO_4$;
   (b) $V_2O_5 + H_2O \rightleftarrows 2HVO_3$.
2. (a) $^*[VO_2]^+ + H_2O \rightleftarrows HVO_3 + {}^*H^+$;
   (b) $^*[VO_2]^+ + 2H_2O \rightleftarrows H_3VO_4 + {}^*H^+$.
3. $H_3VO_4 \rightleftarrows HVO_3 + H_2O$.
4. $HVO_3 + Na^+Y \rightleftarrows NaVO_3 + H^+Y$.
5. $NaVO_3 + H_2O \rightleftarrows HVO_3 + NaOH$.

If vanadium is present as V_2O_5, it will be a liquid at reaction conditions and, as indicated elsewhere (9, 28), will react in steam to give the hydroxy or acid compound. Similarly, if V is in a +5 oxidation state as an adsorbed surface $^*[VO_2]^+$ species, where $*$ is a surface site, it can also react to form an acid. Though we have written reactions to make vanadic and metavanadic acid, the concentrations of the two acids would come to an equilibrium value at reaction conditions. The critical steps for our mechanism are steps 4 and 5. The acid reacts with the sodium cation on the Y zeolite to form sodium metavanadate. And the sodium metavanadate hydrolyzes in steam to give NaOH and metavanadic acid. Again it is immaterial which acid we propose and even complex acids such as $H_4V_2O_7$ (26, 29) have been proposed; metavanadic acid offers the simplest reaction path attacking one Na cation.

Metavanadic acid is a catalyst that facilitates the removal of sodium from its cationic site by forming the reaction intermediate sodium metavanadate, which, as shown in Table 5 and Fig. 8, is quite potent for Y destruction. Once this intermediate hydrolyzes to NaOH (step 5), Y destruction takes place exactly as in the case with no vanadium (pathway B). This is reminiscent of the low-temperature hydrolysis of $NaHCO_3$ to NaOH with consequential Y destruction.

Our UV–visible spectroscopy experiments with model vanadium compounds substantiate the above proposal. In the sodium metavanadate case, we obtain, after steaming, bands at 480 and 290 nm, attributed to oxides of vanadium. This is a clear indication of the separation of Na from V during the steam treatment and validates our proposed mechanism (step 5) in which $NaVO_3$ reacts with steam to form NaOH and HVO_3. We do not observe these bands for vanadium in the case where we used ammonium metavanadate. Here the spectroscopic results for calcined and steamed samples are identical, indicating that the overall vanadium surface structure and composition seem to be the same after calcination and after steaming. This is consistent with our observation that metavanadic–vanadic acid from the ammonium metavanadate plays no role in zeolite destruction.

In the case without vanadium, sodium removal would need to take place by hydrolysis of Na^+Y.

6. $H_2O + Na^+Y \rightleftarrows NaOH + H^+Y$.

This uncatalyzed formation of NaOH we suggest is a difficult step. Therefore due to the catalytic action of V described in steps 4 and 5, the concentration of available NaOH is always greater when vanadium is present.

Destruction of Y zeolite. The mechanism of pathway B for the low temperature case with NaOH and water is straightforward. Here NaOH is solvated and distinct ionic species Na^+ and OH^- form, resulting in the base attack on framework Si–O. In high-temperature steam, 1060 K, there is no solvation or facile formation of ionic species. However in order to attack Si–O and destroy the framework, it is essential to provide a base. We suggest that step 7 takes place with a partial ionization sufficient enough to react in a concerted way with Si–O.

7. $NaOH \xrightarrow{\text{steam}} Na^{\delta+}OH^{\delta-}$.

Steam is essential to the process because without it partial ionization is not possible. The high activation energy of 79 kcal/mol observed by Pine is associated with this sequence of reactions.

It is debatable to what extent sodium silicate, formed after attack of the base on the Si–O bond, will itself hydrolyze to give NaOH and thus continue the destructive event. However, the destruction process is terminated when sodium reacts with Al in USY to form sodium aluminate. We have shown earlier that nonframework Al reacts with Na and thus mitigates destruction.

5. CONCLUDING REMARKS

Our mechanism will hold for vanadium levels up to ca. 1 wt%. At higher V levels, one needs to determine if other pathways for Y destruction are also present. The work we have discussed was carried out on catalysts with no rare

earth or other multivalent cations. However, the same pathways of destruction that we have proposed will be effective for rare earth-containing zeolites. For example, Occelli and Ritz (23) have reported that V, at a level of 4000 ppm, has little affect on a calcined REY zeolite, ucs of 2.4668 nm, containing 0.06 wt% Na_2O. We note that due to the low sodium content of the catalyst, steamed zeolite surface area decreases from 410 m^2/g for vanadium-free catalyst to only 394 m^2/g, a 96% retention even though 4000 ppm V is present. However, high levels of rare earth in the presence of vanadium may introduce another pathway for destruction.

The V-related destructive pathway discussed by previous researchers (9–11) is by hydrolysis of Al_F by acidic vanadium. This pathway would be one that enhances pathway A, hydrolysis via steam, directly. We have shown this pathway to be unimportant. We cannot rule it out completely since catalysts with very low levels of sodium (0.02 wt% Na_2O) still show a small reduction in zeolite surface area in the presence of vanadium. This could, of course, also be the result of the low amount of sodium still being effective. Indeed, one does not need much sodium, if it can be made available with the help of V, to have Y destruction.

Extensive hydrolysis of Al_F would lead to a significant decrease in the unit cell size. Under our steaming conditions, we have not observed differences in ucs when steamed in the presence or absence of V. Under more severe steaming conditions, hydrolysis of Al_F may take place as a secondary process, since the removal of Na^+ via metavanadic acid leaves behind a proton (step 4), thus forming a Si–O–Al site that can be hydrolyzed. In conclusion, we have proposed two distinct pathways leading to Y zeolite destruction. For low Na^+ USY, steam hydrolysis of framework Al is the main cause of zeolite collapse, and there is little effect of V. In the second pathway, sodium is directly responsible for the hydrothermal instability of the zeolite. Sodium from the zeolite combines with steam to generate an active center, a surface $Na^{\delta+}OH^{\delta-}$, for zeolite destruction. When V is present, it facilitates the removal of Na^+ from a zeolite exchange site via an acid–base reaction. The sodium vanadate, or sodium metavanadate, hydrolyzes to $Na^{\delta+}OH^{\delta-}$. Thus in the presence of V, more destructive active centers are formed. The actual destruction of the zeolite via $Na^{\delta+}OH^{\delta-}$ is the same whether V is present or not. This substantiates Pine's (11) observation that the activation energy of destruction is the same whether V is present or not. This unique role of V is not possible with sulfur oxides generated in an FCC regenerator and, as noted by Trujillo *et al.* (10), does not destroy the zeolite.

ACKNOWLEDGMENT

The authors thank Eunice Lambert for her assistance with all the steaming experiments.

REFERENCES

1. Beyerlein, R. A., and McVicker, G. B., *Stud. Surf. Sci. Catal.* **134**, 3 (2001).
2. Beyerlein, R. A., McVicker, G. B., Yacullo, L. N., and Ziemiak, J. J., *in* "Symposium on Fundamental Chemistry of Promoters and Poisons in Heterogeneous Catalysis, New York," Preprints, Vol. 31, p. 190. Am. Chem. Soc., Washington, DC, 1986.
3. Fritz, P. O., and Lunsford, J. H., *J. Catal.* **118**, 85 (1989).
4. Scherzer, J., *Stud. Surf. Sci. Catal.* **76**, 145 (1993).
5. Brown, S. M., Reagan, W. J., and Woltermann, G. M., U. S. Patent 4,325,813 (1982).
6. Pine, L. A., Maher, P. J., and Wachter, W. A., *J. Catal.* **85**, 466 (1984).
7. Madon, R. J., Macaoay, J. M., Koermer, G. S., and Bell, V. A., *in* "12th North American Meeting of the catalysis Society, Lexington, KY," Abstract D33. 1991.
8. Edwards, G. C., Rajagopalan, K., Peters, A. W., Young, G. W., and Creighton, J. E., *ACS Symp. Ser.* **375**, 101 (1988).
9. Wormsbecher, R. F., Peters, A. W., and Maselli, J. M., *J. Catal.* **100**, 130 (1986).
10. Trujillo, C. A., Uribe, U. N., Knops-Gerrits, P.-P., Oviedo, L. A., and Jacobs, P. A., *J. Catal.* **168**, 1 (1997).
11. Pine, L. A., *J. Catal.* **125**, 514 (1990).
12. Liu, X., Truitt, R. E., and Hodge, G. D., *J. Catal.* **176**, 52 (1998).
13. Sohn, J. R., DeCanio, S. J., Lunsford, J. H., and O'Donnell, D. J., *Zeolites* **6**, 225 (1986).
14. Madon, R. J., Koermer, G. S., and Macaoay, J. M., U.S. Patent 5,395,809 (1993).
15. Mitchell, B. R., *Ind. Eng. Chem. Prod. Res. Dev.* **19**, 209 (1980).
16. Centi, G., Perathoner, S., Trifiro, F., Aboukais, A., Aissi, C. F., and Guelton, M., *J. Phys. Chem.* **96**, 2617 (1992).
17. Dzwigaj, S., Matsuoka, M., Franck, R., Anpo, M., and Che, M., *J. Phys. Chem. B* **102**, 6309 (1998).
18. Gates, B. C., Katzer, J. R., and Schuit, G. C. A., "Chemistry of Catalytic Processes." McGraw-Hill, New York, 1979.
19. Gelin, P., and Des Courieres, T., *Appl. Catal.* **72**, 179 (1991).
20. Gelin, P., and Gueguen, C., *Appl. Catal.* **38**, 225 (1988).
21. Breck, D. W., "Zeolite Molecular Sieves." Krieger, Melbourne, FL, 1984.
22. Occelli, M. L., *in* "Catalysis in Petroleum Refining and Petrochemical Industries" (M. Absi-Halabi, *et al.*, Eds.), p. 1. Elsevier, Amsterdam, 1996.
23. Occelli, M. L., and Ritz, P., *Appl. Catal. A* **183**, 53 (1999).
24. Occelli, M. L., and Stencel, J. M., *Stud. Surf. Sci. Catal.* **49B**, 1311 (1993).
25. Catana, G., Rao, R. R., Weckhuysen, B. M., Van Der Voort, P., Vansant, E., and Schoonheydt, R. A., *J. Phys. Chem. B* **102**, 8005 (1998).
26. Occelli, M. L., *Catal. Rev.–Sci. Eng.* **33**, 241 (1991).
27. Anderson, M. W., Occelli, M. L., and Suib, S. L., *J. Catal.* **122**, 374 (1990).
28. Yannopoulos, L. N., *J. Phys. Chem.* **72**, 3293 (1968).
29. Glemser, O., and Muller, A., *Z. Anorg. Allg. Chem.* **325**, 220 (1963).

ELSEVIER

Applied Catalysis A: General 150 (1997) 85–99

APPLIED CATALYSIS A: GENERAL

Effect of sodium deposition on FCC catalysts deactivation

E. Tangstad [a], M. Bendiksen [a,*], T. Myrstad [b]

[a] *SINTEF Applied Chemistry, P.O. box 124 Blindern, N-0314 Oslo, Norway*
[b] *Statoil R&D Centre, Postuttak, N-7005 Trondheim, Norway*

Received 16 April 1996; revised 17 July 1996; accepted 17 July 1996

Abstract

A method for evaluating the sodium tolerance of FCC catalysts by use of a cyclic deactivation unit (CDU) has been developed. In the CDU sodium is impregnated on the catalyst through the introduction of sodium naphthenates into the feedstock during the cracking step. The sodium tolerance of commercial FCC catalysts was studied using this method. Both the amount of added sodium and vanadium were varied to study the effect of increasing metal loading. The deactivated samples were characterised (nitrogen adsorption, elemental analysis, XRD) and tested in MAT. The effect of increasing amounts of sodium on the cracking behaviour of the FCC catalysts was very small compared to the effect of increasing amounts of vanadium. Sodium deposition resulted in a lower activity and less hydrogen transfer reactions, leading to more olefins and less paraffins in the gasoline product. For the commercial FCC catalysts at least 4500 ppm sodium at a level of about 2–2500 ppm vanadium could be applied without changing the cracking characteristics significantly, or without a break-down of the catalyst structure.

Keywords: FCC; Sodium tolerance; Cyclic deactivation; MAT; Resid cracking

1. Introduction

During repeated cycles of cracking, stripping and regeneration the FCC catalyst is exposed to conditions and poisons which result in catalyst deactivation. Metals which are deposited on the catalyst during the cracking reaction are one of the main causes for permanent catalyst deactivation in an FCC unit, and especially in units processing heavy feedstocks. The metals deposited on the

* Corresponding author.

PII S0926-860X(96)00284-0

catalyst are mainly nickel, vanadium and sodium. The effects of nickel and vanadium are quite well known [1,2], whereas the effects of sodium on the catalyst performance have not been investigated to the same extent and the results are not unambiguous. Since sodium is known to deactivate FCC catalysts, it is important to be able to evaluate the catalyst's tolerance for sodium poisoning.

In this work we have looked at the effect of sodium deposited on the catalyst in the FCC unit. In addition to the deposited sodium, the zeolitic part of the FCC catalyst will always contain some sodium from the production of the catalyst. Sodium from the production is ion-exchanged with other cations to different levels in different types of zeolites and catalysts. Too high a level of sodium in the zeolite after production results in low activity and poor hydrothermal stability. Other effects of residual sodium from zeolite production are described in literature [3–5].

Sodium is introduced into the FCC unit through several different routes. The feedstock will contain droplets of brine dispersed in the oil which may originate from the oil production or from water in transportation tanks. The feedstock may also contain solid particles of salt, or remaining production chemicals [6]. In the refinery, salt deposits in lines and tanks can enter the plant when, for example, the tanks are emptied. Processing of slop material in the FCC unit will also be a source for sodium. Failure of the desalter unit can cause carry-over of salt to the FCC unit. Water used in the FCC unit as stripper steam or dispersion steam is also a potential source for sodium.

Various mechanisms have been proposed for catalyst deactivation by sodium poisoning. Deactivation by neutralisation of acid sites is one mechanism which at least can be attributed to sodium left in the zeolite after production, or ion exchanged into the zeolite [3,4,7]. Investigations indicate that sodium will neutralise the strongest acid sites first, causing lower activity and more hydrogen transfer reactions in the catalyst. This would lead to decreasing olefin yields and octane numbers [3,7]. Others claim that sodium only affects catalyst activity and not the product distribution [8,9].

Sodium can also react with the zeolite material and/or vanadium, making an eutectic with a low melting point which will accelerate the hydrothermal deactivation of the catalyst in the regenerator [6,7]. The same reaction with the matrix material will cause the collapse of pore structure and result in lower levels of conversion and higher bottoms yield.

In the laboratory, sodium has generally been added to the catalyst by ion exchange [3,5], mixing with sodium chloride followed by steam treatment [10] or impregnation with different salts [3,9,11]. In this work sodium has been added to the FCC catalyst during the cracking step in a cyclic deactivation unit (CDU), which is more comparable to what happens in a FCC-unit than the methods previously described. Sodium is, together with nickel and vanadium, added to the CDU feed as naphthenates. The purpose of this work has been to evaluate

the combined effects of sodium and vanadium on commercial catalysts designed for cracking of atmospheric residue, and also to evaluate cyclic deactivation as a method for studying sodium tolerance in commercial catalysts.

North Sea atmospheric residue has a sodium level of approximately 1 ppm, resulting in typically 500 ppm additional sodium on the equilibrium catalyst in the RCC unit at Mongstad. For this laboratory work three different levels of sodium added to the catalyst during cyclic deactivation have been chosen, 0/500 ppm additional sodium, representing a low to normal level of sodium on the Ecat (equilibrium catalyst), 2000 ppm additional sodium, representing a high, but realistic level of sodium, and 5000 ppm additional sodium representing a very high level.

2. Experimental

Two commercial resid FCC catalysts which have been considered for use in an RCC-unit, were used in this study. The catalysts will be referred to as CatA and CatB in this paper.

2.1. Cyclic deactivation

Cyclic deactivation of the FCC catalyst was performed in a fully automated cyclic deactivation unit (CDU) [12]. The deactivation conditions of the CDU have previously been adjusted to give test (MAT) results and catalyst characteristics as close to Ecat as possible. The deactivated catalyst was obtained after 35 cycles of cracking, stripping, regeneration and cooling of fresh catalyst. In the cracking step light cycle oil (LCO) was introduced to the catalyst bed at a reaction temperature of 500°C. LCO containing sodium (0–0.299 wt.-% Na), nickel (0.050–0.066 wt.-% Ni) and vanadium (0–0.229 wt.-% V) naphthenates (dissolved in cyclohexane prior to mixing with LCO) was used in the first 30 cycles, while pure LCO was used in the last 5. The boiling point range of the LCO was 185–340°C and it contained 0.07 wt.-% sulphur. During stripping a mixture of nitrogen and steam flowed through the fluidized catalyst bed at increasing temperatures. At 800°C the regeneration step was carried out by passing a mixture of air and steam through the bed, followed by cooling of the catalyst to the cracking temperature. Any remaining coke left on the catalyst samples after deactivation (35 cycles) was removed by calcining at 500°C for 1 h.

For CatA the aim was to obtain 3 levels of sodium (+500, +2000 and +5000 ppm) combined with 3 levels of vanadium (1000, 2500 and 3500 ppm) at a constant nickel level (1000 ppm). For CatB 4 levels of sodium (+0, +1000, +2000 and +5000 ppm) combined with 4 levels of vanadium (0, 1000, 2500 and 3500 ppm) at a constant nickel level (1000 ppm) were desired.

2.2. Elemental analyses

Elemental bulk analyses of sodium, nickel and vanadium were performed with an ICP/AES-instrument following digestion in acid at high temperature and pressure.

Concentration profiles of sodium, nickel and vanadium through catalyst particles were determined using a scanning electron microprobe (EPMA/Cameca Microbeam). Areas of 5×5 μm^2 and a depth of 1.5 μm were used in the measurements.

2.3. Nitrogen adsorption

Nitrogen adsorption was performed with a Carlo Erba Sorptomatic 1800 series. The specific surface area was determined by the BET method, and the matrix surface area was found by using the *t*-plot method.

2.4. UCS

The unit cell size of the zeolite was determined by X-ray diffraction (XRD), based on the standard ASTM D3942-80 procedure.

2.5. Micro activity testing (MAT)

The activity and selectivity of the catalyst after deactivation was measured using the short contact time micro activity test. With some modifications, as described below, the operating conditions were according to ASTM D3907-86. The following definition was used to calculate the conversion:

$$\text{ASTM conversion} = (F - (R \cdot L/100) - H) \cdot 100/F$$

where F = feed (g), R = LCO + DCO in liquid product (wt.-%), L = liquid products (g), H = oil in reactor outlet after reaction (g).

The feed consisted of North Sea atmospheric residue with a boiling point range of 375°C + and with a Conradson carbon residue content of 3.5 wt.-%. In the MAT unit 1 g of feed was injected to the fixed bed reactor during a period of 30 s at a reaction temperature of 524°C. The catalyst/oil ratio varied between 3.5 and 7.5. The reaction products were collected, and the liquid products were quantified and then chromatographically analyzed by simulated distillation (Hewlett Packard 5880) according to the ASTM procedure D-2887. The gaseous products were analyzed with a refinery gas analyzer (Hewlett Packard 5880). The coke on the catalyst surface was subsequently quantified with a CHN analyser. The mass balance, conversion and yields of hydrogen, dry gas ($C_1 + C_2$), LPG ($C_3 + C_4$), gasoline (C_5 up to a boiling point of 216°C), LCO

Table 1
Content of sodium, vanadium and nickel in fresh catalysts

Catalyst	Sodium (wt.-%)	Vanadium (ppm)	Nickel (ppm)
CatA	0.26	80	50
CatB	0.30	45	20

(boiling point range of 216 to 344°C), DCO (boiling point range higher than 344°C) and coke could then be calculated.

The composition of the gasoline fraction was further examined by GC–MS (Finnigan SSQ700) analyses and the software package SI-PIONA from SINTEF [13].

3. Results and discussion

3.1. Sodium, vanadium and nickel addition during cyclic deactivation

Table 1 gives the sodium, vanadium and nickel content of the fresh catalysts, and Table 2 shows the target values for deposition of sodium, vanadium and nickel on the catalyst together with the amounts actually deposited during cyclic deactivation. The amounts of deposited sodium on the CatB samples were calculated by subtraction of the sodium content of CatB-1, where the feed during cyclic deactivation did not contain any sodium. The remaining values of added metals in Table 2 were calculated by subtraction of the metal content in the fresh catalyst from the metal content in the deactivated samples. The results

Table 2
Target amounts of sodium and vanadium in their deposition on the catalysts during cyclic deactivation (Ni = 1000 ppm), and the amounts of sodium, vanadium and nickel deposited (elemental analysis)

Sample	Na (ppm) target	Na (ppm) analysed	V (ppm) target	V (ppm) analysed	Ni (ppm) analysed
CatA-1	500	560	2500	2200	860
CatA-2	2000	1760	2500	2100	790
CatA-3	5000	4460	2500	2100	850
CatA-4	2000	1860	1000	1030	930
CatA-5	2000	2060	2500	2050	950
CatA-6	2000	1860	3500	3300	970
CatB-1	0	0	2500	2060	1140
CatB-2	2000	1480	2500	2360	1010
CatB-3	5000	4540	2500	2380	980
CatB-4	2000	1750	0	80	1030
CatB-5	2000	1960	2500	2730	1210
CatB-6	2000	1970	3500	3340	1110
CatB-7	1000	810	1000	1040	1020

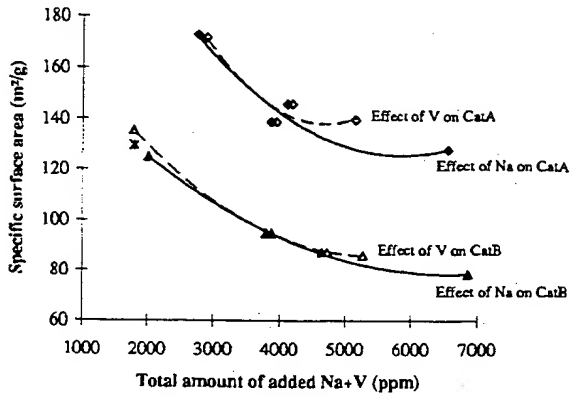

Fig. 1. Total surface area as a function of vanadium and sodium deposited on CatA and CatB during cyclic deactivation. ♦: CatA, changing Na, V = 2000 ppm. ▲: CatB, changing Na, V = 2500 ppm. ◇: CatA, changing V, Na = 2000 ppm. △: CatB, changing V, Na = 2000 ppm. ∗: CatB, Na = 1000 ppm, V = 1000 ppm.

show that the precision of the amounts of sodium added to the catalysts compared to the target values, is at about the same level as the precision of vanadium and nickel additions. The average deviation between target and actually added amounts of sodium in the deactivations of Table 2 is 10.2%.

3.2. Specific surface areas

The total surface area of CatA and CatB had a similar response to the addition of sodium during cyclic deactivation as can be seen in Fig. 1. The decrease in the total surface area per ppm sodium added is greater at low levels of sodium compared to higher levels (2–4500 ppm). Sodium and vanadium affect the total surface area of the catalysts to the same degree. There is a tendency of stabilisation of the surface towards further destruction by high vanadium levels in CatA.

Both the zeolite surface area of CatA and CatB decrease after adding sodium (Fig. 2), but there is no tendency of a structural collapse of the zeolite in either of the catalysts after adding sodium in amounts of up to 4500 ppm combined with 2–2500 ppm vanadium. As can be seen in Fig. 3, sodium does not affect the matrix surface area to the same extent as it affects the zeolite surface area, especially not for CatB where the matrix surface area does not decrease at all even after adding up to 4500 ppm sodium. This is in agreement with Zhao and Cheng [11] who also observed a higher decrease in the zeolite surface area than the matrix surface area (no decrease) as a function of increasing sodium level in the catalyst zeolite after laboratory steam deactivation. The decline in the matrix surface area of different Ecats as a function of total sodium was in the same range as our CatA results.

From Figs. 2 and 3 it can be seen that sodium and vanadium affect the zeolite

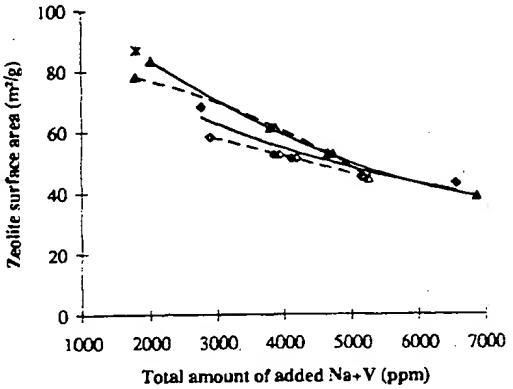

Fig. 2. Zeolite surface area as a function of vanadium and sodium deposited on CatA and CatB during cyclic deactivation. ◆: CatA, changing Na, V = 2000 ppm. ▲: CatB, changing Na, V = 2500 ppm. ◇: CatA, changing V, Na = 2000 ppm. △: CatB, changing V, Na = 2000 ppm. *: CatB, Na = 1000 ppm, V = 1000 ppm.

and matrix surface of the catalysts in different ways: at low metal levels (0–3500 ppm Na + V) the added sodium seems to have a slightly more significant negative effect on the zeolite surface area of the catalysts than a corresponding amount of vanadium has. However, for CatB this difference is at the limit of what can be considered to be significant with respect to the accuracy of the measurements. At these low metal levels the matrix surface areas are reduced more by vanadium than by a corresponding amount of deposited sodium.

It has been claimed that there exists a synergic effect between sodium and vanadium on FCC catalysts [7,14]. In this study specific surface areas of three cyclic deactivated samples of CatB with different ratios between the added

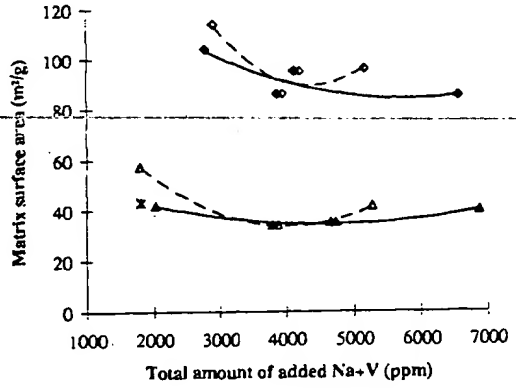

Fig. 3. Matrix surface area as a function of vanadium and sodium deposited on CatA and CatB during cyclic deactivation. ◆: CatA, changing Na, V = 2000 ppm. ▲: CatB, changing Na, V = 2500 ppm. ◇: CatA, changing V, Na = 2000 ppm. △: CatB, changing V, Na = 2000 ppm. *: CatB, Na = 1000 ppm, V = 1000 ppm.

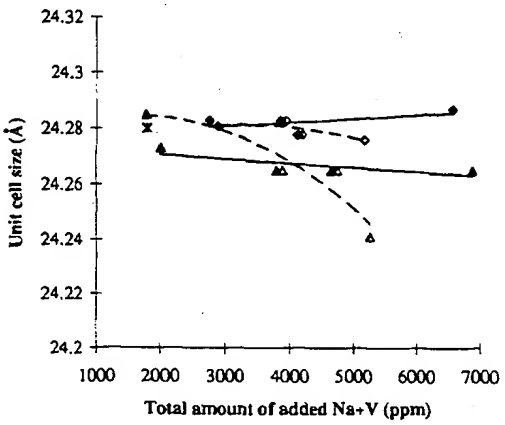

Fig. 4. Unit cell size as a function of vanadium and sodium deposited on CatA and CatB during cyclic deactivation. ◆: CatA, changing Na, V = 2000 ppm. ▲: CatB, changing Na, V = 2500 ppm. ◇: CatA, changing V, Na = 2000 ppm. △: CatB, changing V, Na = 2000 ppm. *: CatB, Na = 1000 ppm, V = 1000 ppm.

sodium and vanadium, but with similar total amounts of the metals, do *not* show such an effect (1000 ppm Na + 1000 ppm V (CatB-7), 2000 ppm Na + 0 ppm V (CatB-4) and 0 ppm Na + 2500 ppm V (CatB-1): the total surface area of CatB-7 has a value *between* CatB-4 and CatB-1, and not a lower value as could be expected if there existed a synergic effect. With an additive effect between added sodium and vanadium, the matrix surface area of CatB-7 could be expected to have a value between CatB-4 and CatB-1, but closest to CatB-1 since sodium has a less significant negative effect than vanadium on the matrix area (Fig. 3). The measurements indicate therefore an additive effect rather than a synergic effect between sodium and vanadium on the matrix surface area. In addition the zeolite surface area measurements do not indicate a synergic effect between the two elements, as the difference of CatB-7 from CatB-1 cannot be resolved within the limits of the experimental accuracy.

3.3. Unit cell size (UCS)

Fig. 4 shows that no significant effects can be observed on the unit cell size of the zeolite in CatA and CatB by addition of sodium in amounts of up to 4500 ppm. Vanadium does not reduce the unit cell size of CatA, while the unit cell size of CatB is reduced by about 0.05 Å after the addition of 3500 ppm vanadium. If sodium does not have a significant effect on the unit cell size (as already shown), it would be expected that a deactivated sample of CatB containing 2000 ppm Na + 1000 ppm V ('CatB-0') would have a similar unit cell size as 1000 ppm Na + 1000 ppm V (CatB-7) if there existed an additive effect between the two metals. A plot of this value for CatB-0 shows a good fit with the plot of CatB at increasing vanadium amounts combined with a constant

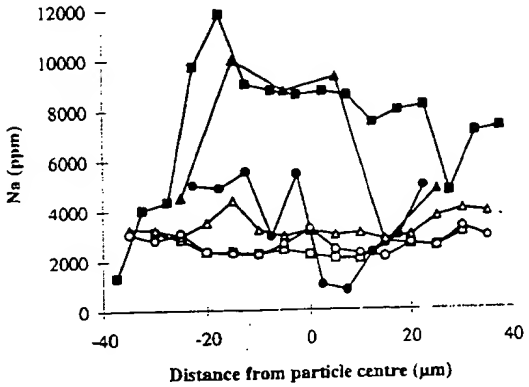

Fig. 5. Sodium distribution through 6 particles of CatA-3.

sodium level (= 2000 ppm), indicating an additive effect between sodium and vanadium rather than a synergic effect on the unit cell size.

3.4. Distribution of sodium, vanadium and nickel in the catalyst particles

The distribution of sodium through six particles of CatA-3 (5000 ppm Na) and through four particles of CatB-3 (5000 ppm Na) is shown in Figs. 5 and 6, respectively. The black labels of Fig. 5 (CatA) represent metal trap particles, while the white labels represent active catalyst particles. CatB does not have separate metal trap particles.

Fig. 5 shows that sodium is distributed quite evenly throughout the active catalyst particles of CatA, and not so evenly distributed through the metal trap particles. The high level of sodium in two of the three metal trap particles and the low level of sodium in the active catalyst particles of Fig. 5 indicates that the metal trap of CatA is also a sodium trap. Sodium is also quite evenly distributed through the four catalyst particles of CatB that were analysed, as is shown in

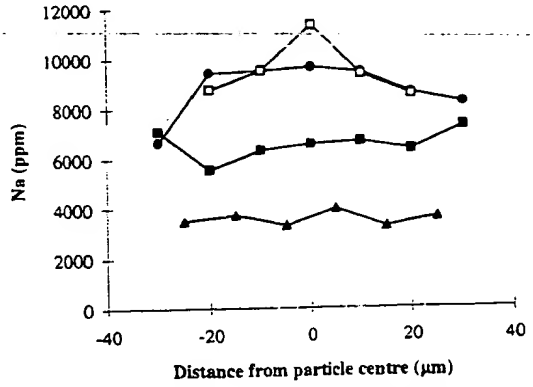

Fig. 6. Sodium distribution through 4 particles of CatB-3.

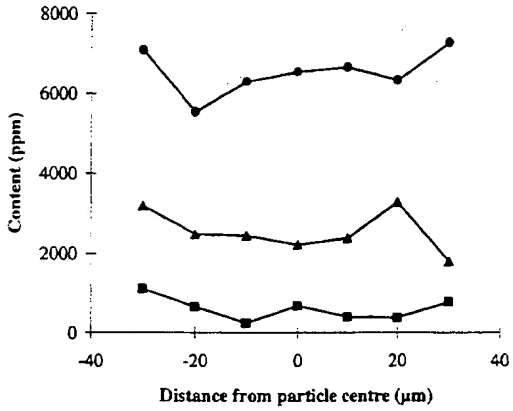

Fig. 7. Nickel (■), vanadium (▲) and sodium (●) distributions through a particle of CatB-3.

Fig. 6. The good distribution of sodium in CatA and CatB is in agreement with Zhao and Cheng [11], who claim that sodium ions move easily within a catalyst particle at regeneration temperatures.

Profiles of both vanadium, nickel and sodium within a particle of CatB-3 are shown in Fig. 7. The profiles of vanadium and nickel vary from particle to particle in both CatA and CatB, and the measurements of these elements in a total of seven active particles from CatA and CatB do not give unambiguous enough results to claim that vanadium is more evenly distributed through the particles than nickel, or the converse.

3.5. Micro activity testing (MAT)

Four samples of cyclic deactivated CatA (CatA-1, -2, -3 and -4) and four samples of cyclic deactivated CatB (CatB-1, -2, -3 and -4) were tested in the MAT unit. Fig. 8 shows the relative catalyst activity (catalyst/oil ratio at 75% conversion) as a function of the total amount of sodium and vanadium deposited

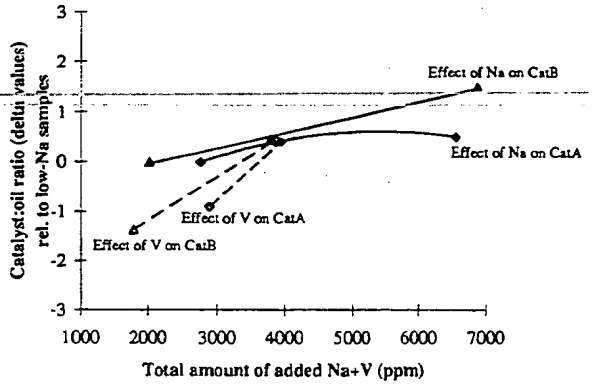

Fig. 8. Catalyst/oil-ratio at 75% conversion as a function of vanadium and sodium deposited on CatA and CatB during cyclic deactivation. ♦: CatA, changing Na, V = 2000 ppm. ▲: CatB, changing Na, V = 2000 ppm. ◇: CatA, changing V, Na = 2000 ppm. △: CatB, changing V, Na = 2000 ppm.

on CatA and CatB during deactivation. There were no signs of overcracking, identified by stable or decreasing gasoline yields by increasing conversion, in the 75% conversion area for these catalyst samples, when using atmospheric residue as feed in the MAT. The catalyst/oil ratios are given as delta values, where the low Na-samples of the two catalysts (CatA-1 and CatB-1) are the reference values. That is: catalyst/oil ratio (delta value) = measured ratio − measured ratio of CatA-1/CatB-1, for CatA and CatB, respectively. To maintain the conversion at 75% when going from 500 to 5000 ppm sodium loaded on the catalyst, it is necessary that an increase of the catalyst/oil ratio of about 10% for CatA or about 20% for CatB is made. At up to 2000 ppm added sodium, the activity change is rather similar for the two catalysts, while from 2000 to 5000 ppm added sodium the activity of CatA is less affected than the activity of CatB.

The activity loss by changing the amount of vanadium from 0 ppm/1000 ppm to 2000 ppm is considerably higher than the effect of a corresponding increase in the sodium levels for both CatA and CatB.

The cyclic deactivated samples of CatA and CatB containing no or little vanadium (2000 ppm Na + 0 ppm V = CatB-4 or 2000 ppm Na + 1000 ppm V = CatA-4) have a higher activity than the samples containing no or little added sodium (0 ppm Na + 2500 ppm V = CatB-1 or 500 ppm Na + 2500 ppm V = CatA-1), despite the fact that the aforementioned samples have a lower zeolite/matrix ratio. The CatB samples have similar zeolite surface areas, while CatB-4 has a higher matrix surface area than CatB-1. With an active matrix of CatB, it is then not unexpected to have a higher activity of CatB-4. A larger unit cell size of CatB-4 compared to CatB-1 may also be a contributory factor to the different activities of the samples. The lower zeolite/matrix ratio of the CatA sample with sodium and little vanadium (CatA-4), is due both to a lower zeolite surface area and a higher matrix surface area, compared to the CatA sample with vanadium and little sodium (CatA-1). For this reason it seems that the matrix surface area of CatA affects the conversion level more than the zeolite surface area, that is a high matrix surface area has a positive effect upon the activity of the CatA. Other factors that do not affect the surface area or the unit cell size may of course also influence the activity of the catalyst, leading to a higher activity of the samples where only sodium is deposited compared to the samples where only vanadium is deposited. It is claimed, for instance, that sodium neutralises acid sites in the zeolite. This could be one reason why increasing sodium loading decreases the activity, but this could not explain why impregnated sodium affects the activity to a lesser extent than vanadium. Infrared (IR) measurements after pyridine adsorption does not indicate any general correlation between the number of Brønsted/Lewis sites or the Brønsted/Lewis sites ratio of the sodium and vanadium loaded CatB samples and MAT activity.

An increasing sodium level of CatA and CatB does not affect the hydrogen production significantly, whereas the hydrogen yield clearly increases with

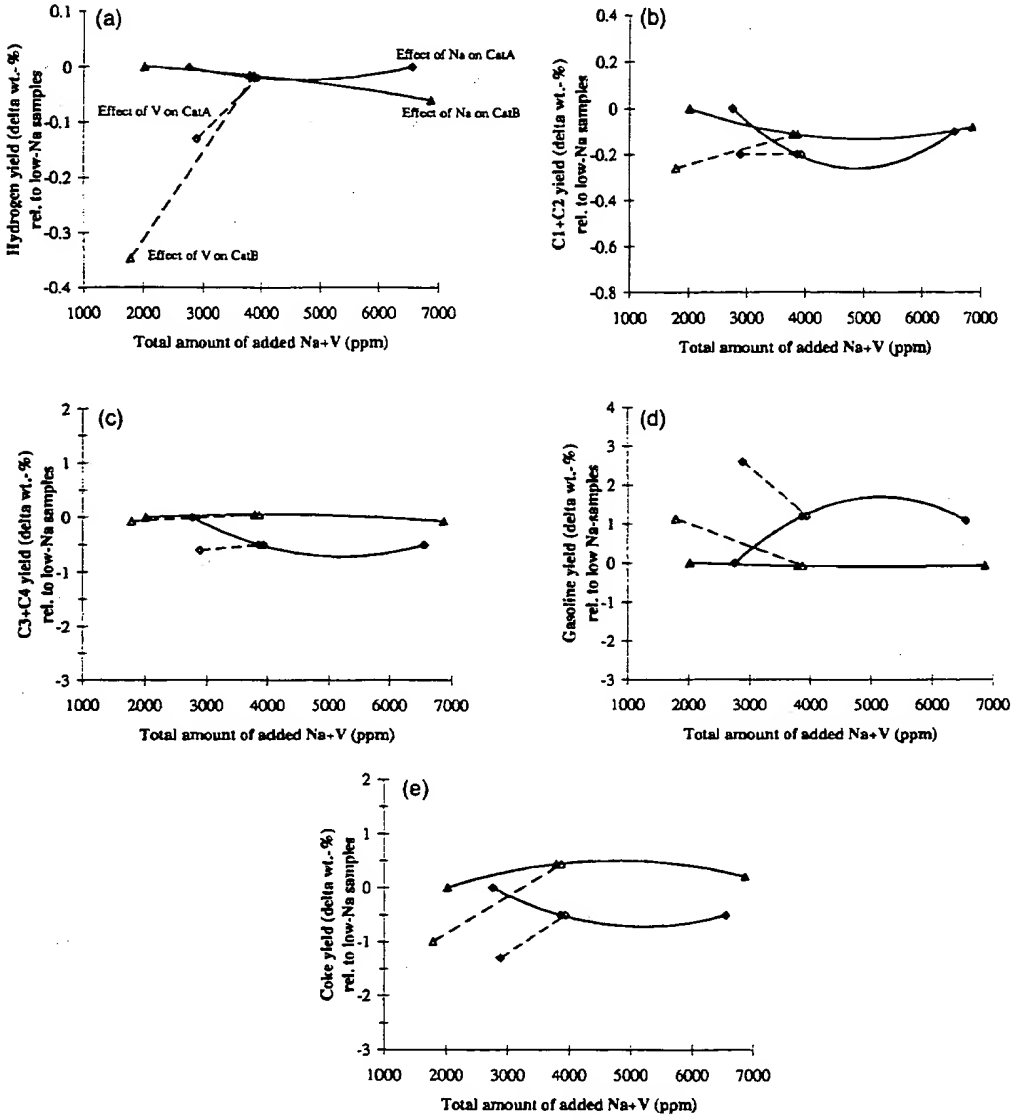

Fig. 9. Product distribution at 75% conversion as a function of vanadium and sodium deposited on CatA and CatB during cyclic deactivation. (a) Hydrogen yield, (b) dry gas yield, (c) LPG, (d) gasoline and (e) coke. ◆: CatA, changing Na, V = 2000 ppm. ▲: CatB, changing Na, V = 2000 ppm. ◇: CatA, changing V, Na = 2000 ppm. △: CatB, changing V, Na = 2000 ppm.

increasing vanadium loading (Fig. 9a). The delta yield values given in Fig. 9 are calculated by the same procedure as described above for Fig. 8.

As the additional sodium loading is increased up to 2000 ppm the dry gas yield ($C_1 + C_2$) decreases to some extent, while a corresponding increase in the vanadium loading does not influence the dry gas production significantly (CatA) or lead to a certain increase in the dry gas production (CatB). From 2000 to 4500 ppm added sodium the dry gas yield does not change (Fig. 9b).

In Fig. 9c a similar trend can be seen in the production of LPG ($C_3 + C_4$) from CatA, however, the changes in LPG as a function of sodium or vanadium levels are small. Neither an increase in added sodium or vanadium on CatB influence the production of LPG significantly.

The gasoline yield from CatA increases with an increase in the sodium loading from 500 to 2000 ppm, while the gasoline yield from CatB is unchanged up to 2000 ppm added sodium (Fig. 9d). The gasoline production is unchanged from 2000 to 5000 ppm sodium for both catalysts. Adding up to 2000 ppm vanadium leads to a decrease in the gasoline yield for CatA and CatB.

Increasing sodium levels do not affect the LCO and DCO yields. An increasing *vanadium* level from 1000 to 2000 ppm does not affect the LCO and DCO yields from CatA, whereas vanadium to a greater extent affects these yields for CatB: the LCO/DCO ratio increases with increasing amounts of vanadium deposited.

For CatA the coke yield decreases somewhat from 500 to 2000 ppm added sodium, while the coke yield from CatB increases somewhat up to 2000 ppm sodium (Fig. 9e). More than 2000 ppm added sodium does not change the coke yield for either of the catalysts. At increasing vanadium levels the production of coke increases for both CatA and CatB.

The results show several similarities in how CatA and CatB respond to increasing amounts of added sodium and vanadium. Increased sodium loadings from 2000 to 4500 ppm do not change the yield structure from either of the two catalysts at a level of 2500 ppm vanadium, whereas an increasing vanadium level (up to 2000 ppm) at a constant level of added sodium of 2000 ppm, clearly has a more negative impact on the product distribution than an increasing sodium level. This results in higher hydrogen and coke production and less gasoline for both CatA and CatB.

An increase in the sodium level from 500 to 2000 ppm of CatA has a positive effect on the yield structure with a lower gas and coke production and a higher gasoline yield, which is probably caused by overcracking of the gasoline when using the low sodium loaded catalyst, due to a high zeolite/matrix ratio in this sample. A further increase in the amount of sodium on this catalyst leads to more unconverted gasoline and so the product distribution will be improved. The change in product distribution after increasing the sodium loading from 0 to 2000 ppm of CatB is less significant compared to the change in the product distribution of CatA.

The composition of the gasoline fraction of the liquid products from testing cyclic deactivated CatA and CatB with different sodium levels (0/500 ppm, 2000 ppm and 5000 ppm Na) is given in Table 3. At increasing sodium levels the paraffin (n- and iso-paraffins) and aromatic content of the gasoline fraction decreases for both CatA and CatB, while the olefin content increases. The calculated RON values do not change significantly.

There are also some differences in how the product quality is affected by

Table 3
Gasoline quality at a catalyst/oil ratio of 5.5

Catalyst sample	Na target (ppm)	Conv. (%)	N-paraffins (wt.-%)	Iso-paraffins (wt.-%)	Olefins (wt.-%)	Napthenes (wt.-%)	Aromatics (wt.-%)	Calculated RON/MON
CatA-1	500	77.7	4.8	26.4	21.3	10.1	37.0	87.6/76.7
CatA-2	2000	75.5	4.1	24.6	24.9	10.8	35.0	87.5/76.8
CatA-3	5000	74.7	4.3	24.4	25.2	11.0	34.7	87.3/76.6
CatB-1	0	73.9	4.3	28.2	21.0	9.6	36.8	88.0/77.8
CatB-2	2000	72.4	4.1	27.8	23.4	9.3	35.1	87.8/77.3
CatB-3	5000	67.4	4.1	25.9	26.8	9.4	33.4	87.6/76.7

sodium during testing of CatA and CatB: the calculated MON values decreases somewhat with increasing sodium for CatB, while these values are unchanged for CatA, and the naphthene and the n-paraffin content of the gasoline from CatB are not affected as much by added sodium as the corresponding values from CatA. These differences are, however, small compared to the similarities in the sodium response of CatA and CatB.

The changes in gasoline composition as a function of increasing amounts of sodium impregnated on the catalysts indicate less hydrogen transfer reactions during testing. The observed effect corresponds well with the effect one may observe at a higher extent of dealumination in the zeolite, which leads to a change in the product composition towards more olefins and naphtenes, and less paraffins and aromatics. Hydrogen transfer reactions also leads to increased coke production, which may explain why the coke yield decreases when testing CatA with increasing sodium loading. Less hydrogen transfer reactions with increasing sodium loadings are not in agreement with Reagan et al., and Witoshkin [3,7] who claim that sodium will lead to *more* hydrogen transfer reactions due to poisoning of the strongest, zero next nearest nabour (0NNN), acid sites.

The fresh sample of CatA has a higher content of rare earth metals, a larger unit cell, higher surface area and a higher zeolite content than CatB. Due to these differences it is not surprising that the two catalysts show different response to metal poisoning. A more active CatA, due to higher surface area and higher zeolite content, might explain why the product distribution is improved from CatA by addition of 2000 ppm sodium and not in CatB. By addition of sodium CatA reach a more optimal activity level for the feed used in these experiments. The similarities in the two catalyst's response to sodium and vanadium poisoning is, however, much more distinctive than expected when starting this work.

4. Conclusions

A method for adding sodium during cyclic deactivation has been developed. The precision of the amount of added sodium is at the same level as the corresponding precision of vanadium and nickel addition.

Sodium deposited on two commercial resid catalytic cracking catalysts gave only small changes in cracking characteristics compared to vanadium impregnation. Sodium amounts up to at least 4500 ppm may be applied at a constant level of 2–2500 ppm vanadium without a further breakdown of catalyst structure or cracking characteristics. Deposited sodium led to more olefins and less paraffins in the gasoline product (less hydrogen transfer reactions).

Even though similarities in how the two catalysts react on increasing sodium loading dominate, there are some differences in the cracking behaviour between the two catalysts. For example the activity is not equally affected by sodium at higher loadings and the product distribution is not equally affected by low sodium loadings.

No significant structural synergic effects have been found between sodium and vanadium deposited on CatB.

Acknowledgements

The authors are grateful to Statoil for the permission to publish this work. B.M. Hustad, J. Simensen, B. Sortland, A.I. Spjelkavik and K. Urdal are acknowledged for their laboratory work contributions.

References

[1] J.S. Magee and M.M. Mitchell Jr., Stud. Surf. Sci. Catal., 76 (1993) 339.
[2] M.L. Ocelli, Fluid Catalytic Cracking, Role in Modern Refining (ACS Symp. Ser., Vol. 375), 1987, p. 182.
[3] W.J Reagan, G.M. Waltermann and S.M. Brown, Prepr. ACS, Div. Petr. Chem., Symp. on Advances in Catalytic Cracking, Washington DC, Aug. 28–Sep. 2, 1983, pp. 884–893.
[4] A. Corma and B. Wojciechowski, Catal. Rev. Sci. Eng., 24(1) (1982) 1–65.
[5] L.A. Pine, P.J. Maher and W.A. Wachter, J. Catal., 85 (1984) 466–476.
[6] W.S. Letzsch and D.N. Wallace, Oil Gas J., Nov. 29 (1982) 58–68.
[7] A. Witoshkin (Engelhard Corp.), Petroleum Catalysts and Process Seminar, Geneva, Switzerland, Sep. 1988.
[8] R.E. Ritter, J.E. Crighton, T.G. Roberie, D.S. Chin and C.C. Wear, Catalytic Octane from the FCC, NPRA ann. meeting, Los Angeles, CA, Mar. 23–25, 1986.
[9] D.R. Forester, US patent no. 5,019,241 (1991).
[10] F. Mauge, P. Gallezot, J.C. Courcelle and J. Grosmangin, Zeolites, 6 (1986) 261–266.
[11] X. Zhao and W.-C. Cheng, Prepr. ACS, Div.Petr.Chem., Symp. on Deactivation and Testing of Hydrocarbon Conversion Catalysts, Chicago, Aug. 20–25, 1995, pp. 406–411.
[12] M. Bendiksen, E. Tangstad and T. Myrstad, Appl. Catal. A, 129 (1995) 21–31.
[13] S.T. Teng, A.D. Williams and K. Urdal, J. High Res. Chromatogr., 17 (1994) 469–476.
[14] L.A. Pine, J. Catal., 125 (1990) 514–524.